Journal of Alloys and Compounds 505 (2010) 783–786

Contents lists available at ScienceDirect

Journal of Alloys and Compounds

journal homepage: www.elsevier.com/locate/jallcom

# Dielectric properties of Mg-doped $Ba_{0.6}Sr_{0.4}TiO_3$ ceramics prepared by using sol–gel derived powders

Jiangying Wang[a,*], Jingji Zhang[a], Xi Yao[b]

[a] College of Material Science and Engineering, China Jiliang University, Hangzhou 310018, China
[b] Functional Materials Research Laboratory, Tongji University, Shanghai 200092, China

ARTICLE INFO

*Article history:*
Received 9 April 2010
Received in revised form 20 June 2010
Accepted 22 June 2010
Available online 1 July 2010

*Keywords:*
Sol–gel synthesis
Differential scanning calorimetry
Dielectric properties

ABSTRACT

Structural and dielectric properties of $y$MgO–$(1-y)Ba_{0.60}Sr_{0.40}TiO_3$ (BST) (where $y$ = 3, 5, 10, 20, 30 and 40 mol%) ceramics prepared by using sol–gel derived powders have been investigated. It is found that a careful control of the synthesis process enables producing a pure perovskite BST phase at a relatively low calcining temperature of 600 °C. Two phases, corresponding to BST and MgO phases, are clearly visible when MgO content up to 20 mol%. The influence of MgO additive on dielectric properties of BST ceramics can be classified into two categories: one is the substitution effect of $Mg^{2+}$ ions and the other is the "composite" effect of MgO.



## 1. Introduction

In the past decades, barium strontium titanate ($Ba_{1-x}Sr_xTiO_3$, BST) ferroelectric materials have attracted increasing research interest due to its strong dielectric nonlinearity under bias electric field. BST with low dielectric loss and high tunability is a promising candidate material in tunable microwave dielectric devices, such as tunable mixers, filters and phase shifters [1–3]. Ferroelectric and dielectric properties of BST ceramics are strongly dependent on the sintering conditions, grain size, porosity, doping amount and structural defects. It is implied that proper doping and sintering conditions may be a promising way to improve the dielectric properties of BST ceramics [4]. Conventional solid-state reaction is not suitable for preparing BST powders with high performance, due to their high calcined temperature (900–1100 °C) [5,6]. Hence, it is necessary and important to adopt other methods to synthesize BST powders with desired microstructure and properties. The sol–gel process has been proved to be very effective at producing ceramics powders of high purity, small size and good uniformity at relatively low sintering temperature [7,8]. In addition, it is reported that additive, such as MgO [9,10] and $MgTiO_3$ [11,12], could be used to improve the permittivity and loss tangent of BST ceramics.

In this study, the main purpose is to prepare Mg-doped $Ba_{0.60}Sr_{0.40}TiO_3$ ceramics by using sol–gel derived powders, and then to analyze the effect of the concentration of MgO doping on their structure and dielectric properties.

## 2. Experimental

$y$MgO–$(1-y)Ba_{0.60}Sr_{0.40}TiO_3$ (where $y$ = 3, 5, 10, 20, 30 and 40 mol%) ceramics were prepared by using sol–gel derived powders. Starting materials were barium nitrate ($Ba(NO_3)_2$), strontium nitrate ($Sr(NO_3)_2$), tetrabutyl titanate ($Ti[O(CH_2)_3CH_3]_4$), magnesium nitrate ($Mg(NO_3)_2$) and citric acid. The nominal amounts of $Ba(NO_3)_2$, $Sr(NO_3)_2$, and $Mg(NO_3)_2$ powders were first dissolved in appropriate amounts of $H_2O$ and citrate acid stirred at 90 °C until the solution became transparent and cooled it down to room temperature. $Ti[O(CH_2)_3CH_3]_4$ solution was added in an appropriate amounts of citric acid by stirring at 50–60 °C. After the above solution turned clear, the Ba–Sr–Ti–Mg–O solution was prepared by mixing titanium solution and barium, strontium, and magnesium solution stoichiometrically. The resulting Ba–Sr–Ti–Mg–O solution became transparent sols at 50–60 °C and then formed gels at 80–90 °C. Thermal decomposition of gels was conducted at a heating rate of 10 °C/min in flowing air, at 750 °C, in an $Al_2O_3$ boat, and cooled it to room temperature. Small BST crystallites were formed in these firing processes. The fired gels were then crushed and ground by ball mill with ethanol for 24 h to obtain fine ceramic powders. The fine ceramic powders were pressed into disc-shaped pellets with a diameter of 10 mm. No binder was used. The pellets were subsequently sintered at 1200–1300 °C for 2 h in air. The compositions with $y$ = 3, 5, 10, 20, 30 and 40 mol% are termed as Sample BSTM03, BSTM05, BSTM10, BSTM20, BSTM30, and BSTM40, respectively.

A differential thermal analysis (DSC/TG/DTG) (Model Netzsch STA449C, Germany) was performed for the Ba–Sr–Ti–Mg gels to investigate their thermal decomposition behavior. Bulk density of Mg-doped $Ba_{0.60}Sr_{0.40}TiO_3$ ceramics was measured by the Archimedes method using distilled water as liquid medium. Powder X-ray diffraction (XRD) measurements were carried out to examine the crystal structure of BSTM powders and ceramics. An X-ray powder diffractometer (Model Rigaka D/max 2550pc, Japan) was used with CuKα radiation at 18 kW and scan rates of 4°/min and from 20–60° ($2\theta$). Scanning electron microscopy (SEM, Model JEOL-5510LV, Japan) was used to characterize the samples' microstructures. Silver paste was added to both faces of the disks, which were then fired at 600 °C as electrodes. Permittivity and loss tangent as functions of temperature were measured at 100 kHz using a programmed HP 4284A precision LCR meter (Agilent, Palo Alto, CA). All electrical measurements were performed at a relative humidity of about 60%.

* Corresponding author. Tel.: +86 571 86875609.
*E-mail address:* wjyliu@163.com (J. Wang).

0925-8388/$ – see front matter © 2010 Elsevier B.V. All rights reserved.
doi:10.1016/j.jallcom.2010.06.140

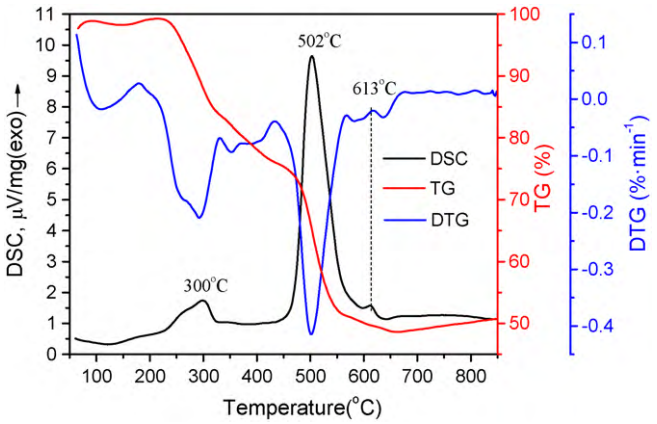


**Fig. 1.** DSC/TG/DTG curves of Ba–Sr–Ti–Mg gel.

## 3. Results and discussion

The thermal analysis results of the Ba–Sr–Ti–Mg gel are shown in Fig. 1. The DSC/TG curves show a weight loss of ~50%, accompanied by three exothermic peaks at 300, 502 and 613 °C. Weight loss at a temperature below 600 °C is attributed to the evaporation of the solvent and the decomposition of organic complex. A faint exothermic peak occurred at ~613 °C, accompanied by a small weight loss of ~1%. This is considered to be caused by the decomposition of residual oxycarbonate of barium and strontium [4]. No further DSC peak or weight loss can be seen thereafter. The XRD patterns for BSTM10 powders annealed in air for 2 h at different temperature are shown in Fig. 2. The XRD results show that amorphous solid is formed at 500 °C, and the BST phase is formed at 600 °C. The BST phase at 600 °C is in cubic structure, and there is no existence of a secondary phase. The diffraction peak of BST ceramic powders become sharp with annealing temperature increasing. The phase development of the powder with increasing annealing temperature is basically consistent with the analysis of the DSC/TG/DTG curves in Fig. 1. The synthetic temperature of $Ba_{0.60}Sr_{0.40}TiO_3$ phase is much lower than that of the conventional solid reaction method [5,6].

The XRD patterns of all samples sintered at 1250 °C are shown in Fig. 3. The samples with low MgO levels ($y \leq 0.10$) are all single-phase BST, whereas those with high MgO levels ($y \geq 0.20$) have additional diffraction lines, assigned to MgO (according to JCPDS

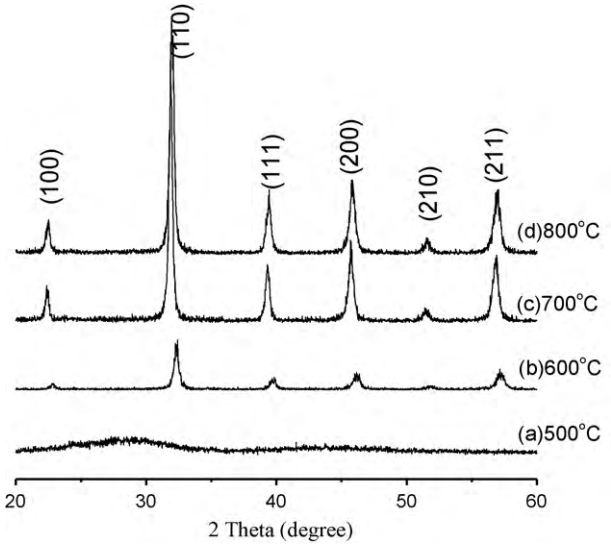


**Fig. 2.** XRD patterns for BSTM10 ceramic powder calcining at different temperature.

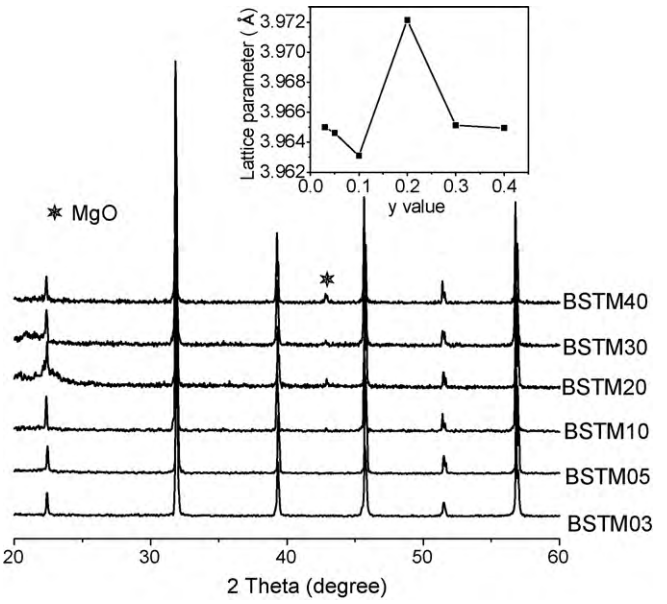


**Fig. 3.** XRD patterns of Mg-doped $Ba_{0.60}Sr_{0.40}TiO_3$ ceramics sintered at 1250 °C for 2 h. The inset presents the lattice parameter variations with $y$ for Mg-doped $Ba_{0.60}Sr_{0.40}TiO_3$ ceramics.

45-0946). It indicates that the solubility of MgO in BST is less than 20 mol%, which is similar to the result reported by Yoon et al. [13].

In addition, the shift of diffraction peaks is not obvious with increasing the MgO content. The lattice parameters for various unit cell of BST were calculated from XRD results, as shown in the inset of Fig. 3. The value of unite cell parameter initially decreases and then increases when $y$ up to 0.20. At $y \leq 0.10$, the lattice parameter of Mg-doped $Ba_{0.60}Sr_{0.40}TiO_3$ ceramics decreases with increasing $y$, all of which is smaller than that of pure $Ba_{0.60}Sr_{0.40}TiO_3$ (3.9650 Å) [14]. Considering the difference of charge and ionic radius among $Ba^{2+}/Sr^{2+}$, $Ti^{4+}$ and $Mg^{2+}$ ions, $Mg^{2+}$ ions can occupy both A- and B-site of BST lattice. It was ever observed that $Mg^{2+}$ ions initially enter into A-site of BST, then into B-site when the $Mg^{2+}$ concentration exceeds 5 mol% in the BST and up to the solubility limit (~15 at.%) [13]. In cubic perovskite $ABO_3$ structure, the coordination number of the A- and B-site is, respectively, 12 and 6. The ionic radius of $Mg^{2+}$ ions (1.03 Å) in 12-fold coordination is smaller than that of $Ba^{2+}$ and $Sr^{2+}$ ($Ba^{2+}$ = 1.61 Å, $Sr^{2+}$ = 1.58 Å) [15], which lead to shrinkage of the crystal cells. It indicates that $Mg^{2+}$ ions mainly substitute for $Ba^{2+}$ or/and $Sr^{2+}$ ions. For the samples with $0.20 \geq y > 0.10$, the lattice parameter is bigger than that of pure BST, due to $Mg^{2+}$ substitution for $Ti^{4+}$ ions. The ionic radius of $Mg^{2+}$ ions (0.72 Å) in 6-fold coordination is bigger than that of $Ti^{4+}$ (0.605 Å) [15], which are responsible for lattice expansion. However, the lattice parameter decreases again when $y > 0.2$, which may be caused by an increase in internal stress with increasing the grain size of BST.

Fig. 4 gives the SEM pictures of Mg-doped $Ba_{0.60}Sr_{0.40}TiO_3$ ceramics sintered at different temperature in air for 2 h. All samples exhibit quite dense microstructure. As the concentration of MgO increases, the grain size of BST reduces, indicating that MgO can suppress the grain growth of BST. The samples with $y > 0.20$ can be sintered well at 1200 °C, which is lower than that of pure $Ba_{0.60}Sr_{0.40}TiO_3$ ceramics [5,6]. Fig. 5 gives relative density variations with $y$ for Mg-doped $Ba_{0.60}Sr_{0.40}TiO_3$ ceramics sintered at 1200, 1250 and 1300 °C. The density of all samples is above 90% of the theoretical value and the relative density increases with increasing sintering temperature. The relative density suddenly drops at $y = 0.20$, which should be close relation to porosity. For the sample with $y = 0.20$, large numbers of oxygen vacancies

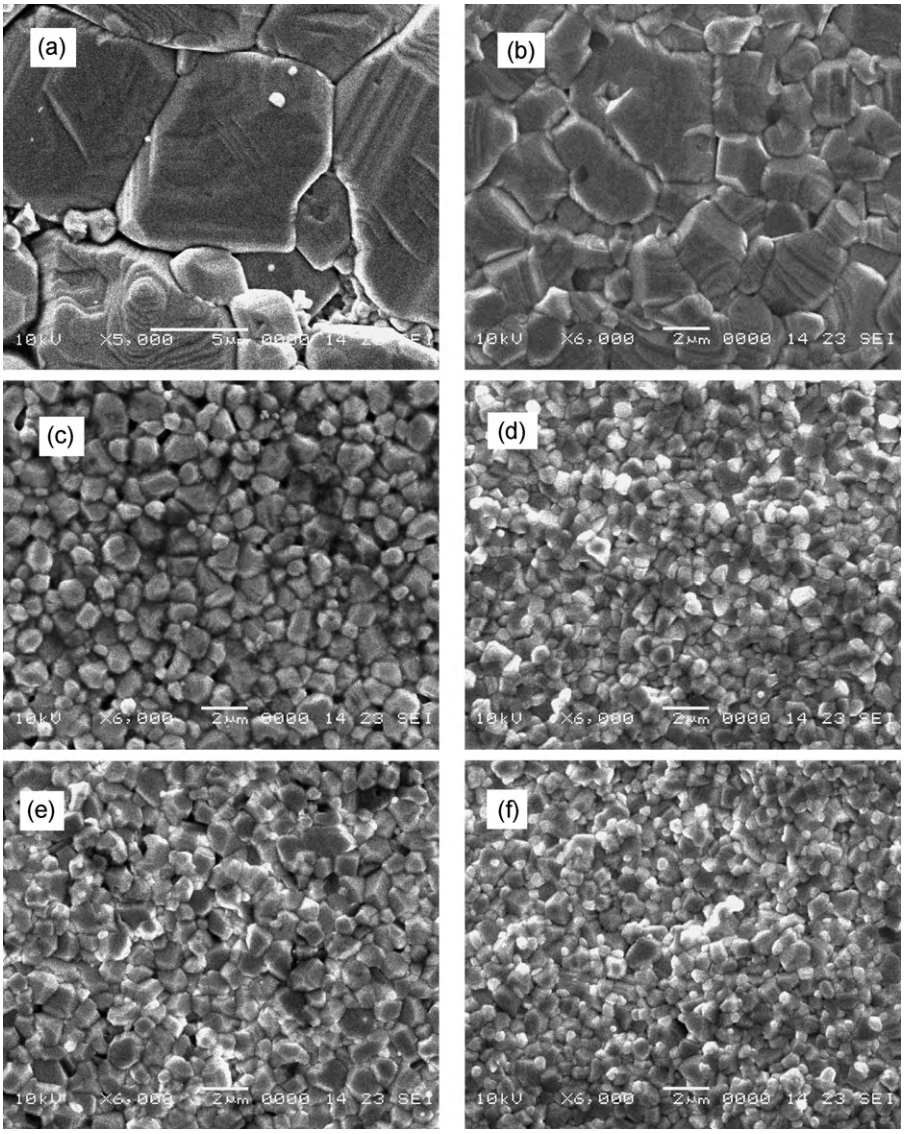


**Fig. 4.** SEM images for the Mg-doped $Ba_{0.60}Sr_{0.40}TiO_3$ ceramics sintered at different temperature in air for 2 h. (a) BSTM03 1300 °C; (b) BSTM05 1300 °C; (c) BSTM10 1200 °C; (d) BSTM20 1300 °C; (e) BSTM30 1200 °C; (f) BSTM40 1200 °C.

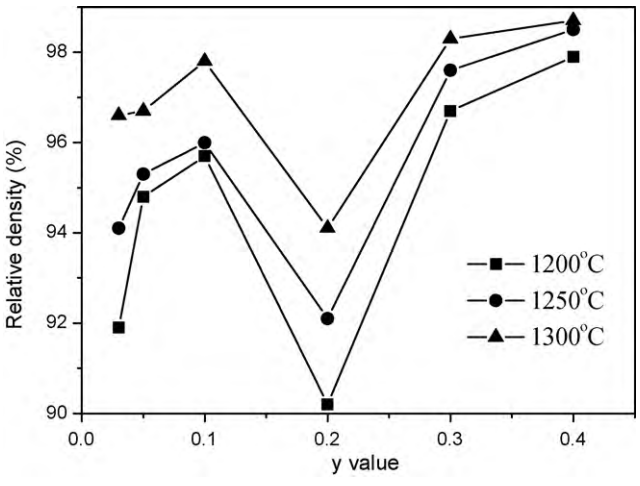


**Fig. 5.** Relative density variations with $y$ for Mg-doped $Ba_{0.60}Sr_{0.40}TiO_3$ ceramics sintered at different temperature for 2 h.

($V_O^{\bullet\bullet}$) are formed by $Mg^{2+}$ substitution for $Ti^{4+}$ ions [16], i.e., $MgO(-TiO_2) \rightarrow Mg_{Ti}^{''} + V_O^{\bullet\bullet} + O_O$. The move of those oxygen vacancies need consume a lot of energy during the sintering process, which causes the decrease of the grain size and the increase of porosity.

Temperature dependences of dielectric permittivity and loss tangent of pure and Mg-doped $Ba_{0.60}Sr_{0.40}TiO_3$ ceramics measured at 100 kHz are presented in Fig. 6. The effect of the concentration of MgO on dielectric permittivity of BST can be clearly seen from Fig. 6a. Compared with pure BST ceramics, the dielectric anomalous peaks of the Mg-doped BST ceramics, corresponding to the cubic-tetragonal phase transitions, are all markedly suppressed and broadened. The suppression and broadening become increasingly pronounced as the concentration of MgO increases. The influence of MgO additive on dielectric properties of $Ba_{0.6}Sr_{0.4}TiO_3$ ceramics can be classified into two categories. At low MgO concentration ($y < 0.20$), the dielectric permittivity, loss tangent and Curie temperature ($T_C$) decrease with increasing the concentration of MgO, which is the substitution effect of $Mg^{2+}$ ions. The reduction in the permittivity is due to the lower polarizability of $Mg^{2+}$ ionic ($0.094 \times 10^{-30}\,m^3$) as compared to that of $Ba^{2+}$,

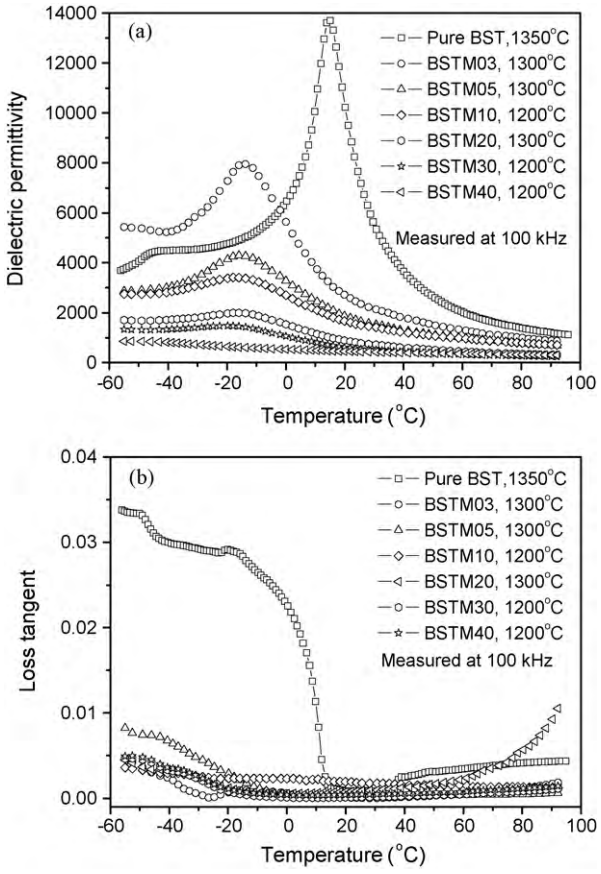


**Fig. 6.** Temperature dependent permittivity and loss tangent for pure BST and Mg-doped $Ba_{0.60}Sr_{0.40}TiO_3$ ceramics sintered at different temperature in air for 2 h.

$Sr^{2+}$, and $Ti^{4+}$ ($Ba^{2+} = 1.550 \times 10^{-30}$ m$^3$, $Sr^{2+} = 0.864 \times 10^{-30}$ m$^3$, and $Ti^{4+} = 0.185 \times 10^{-30}$ m$^3$) [17]. The internal stress may cause the shift of $T_C$. The internal stress increases as the grain size decreases and leads to the shift of $T_C$ toward lower temperature [18]. Another possible explanation for the decrease in $T_C$ [19] and the permittivity maxima is that a high level of Mg substitution deteriorates the ferroelectric long-range order. $Mg^{2+}$ substitution for $Ti^{4+}$ ions can result in the formation of oxygen vacancies, which can suppress the formation of $Ti^{3+}$ to improve the loss tangent. As shown in Fig. 6b, the small increase of loss tangent at high temperatures can be caused by the increase of conduction with increasing temperature. However, for the samples with $y \geq 0.20$, the permittivity and loss tangent further decrease with increasing the concentration of MgO, whereas variation in $T_C$ is not obvious, indicating the "composite" effect of MgO. MgO precipitates out and deteriorates the connection of BST grains, which "dilutes" the permittivity and decreases the domain-wall contribution to the loss tangent.

## 4. Conclusions

$y$MgO–$(1-y)Ba_{0.60}Sr_{0.40}TiO_3$ ($y$ = 3, 5, 10, 20, 30 and 40 mol%) ceramics were prepared by using sol–gel derived powders. For Ba–Sr–Ti–Mg gels, BST phase can be obtained by annealing at 600 °C for 2 h, accompanied by a weight loss of ~50%. The synthetic temperature of $Ba_{0.60}Sr_{0.40}TiO_3$ phase is much lower than that of the conventional solid reaction method. Two phases, corresponding to BST and MgO phases, are clearly visible for the compositions with $y \geq 0.10$. The density of all samples is above 90% of the theoretical value. The effect of MgO additive on dielectric properties of $Ba_{0.6}Sr_{0.4}TiO_3$ ceramics can be classified into two categories: one is the substitution effect of $Mg^{2+}$ ions and the other is the "composite" effect of MgO. MgO precipitates out and deteriorates the connection of BST grains, which "dilutes" the permittivity and decreases the loss tangent.

## Acknowledgement

This work was financially supported by the Ministry of Sciences and Technology of China through 973-project under grant 2009CB623302.

## References

[1] A.K. Tangantsev, V.O. Sherman, K.F. Astafiev, J. Venkatesh, N. Setter, J. Electroceram. 11 (2003) 5–66.
[2] F.D. Flaviis, N.G. Alexopoulos, O.M. Stafosudd, IEEE Trans. Microw. Theory Tech. 45 (1997) 963–969.
[3] E.A. Nenasheva, A.V. Kanareykin, N.F. Kartenko, A.I. Ddeyk, S.F. Karmanenko, J. Electroceram. 13 (2004) 235–238.
[4] Q. Xu, X.F. Zhang, Y.H. Huang, W. Chen, H.X. Liu, M. Chen, B.H. Kim, J. Alloys Compd. 485 (2009) L16–L20.
[5] X.S. Wang, L.L. Zhang, H. Liu, J.W. Zhai, X. Yao, Mater. Chem. Phys. 112 (2008) 675–678.
[6] N.C. Pramanik, N. Anisha, P.A. Abraham, N. Rani Panicker, J. Alloys Compd. 476 (2009) 524–528.
[7] W. Li, Z.J. Xu, R.Q. Chu, P. Fu, J.G. Hao, J. Alloys Compd. 499 (2010) 255–258.
[8] J.W. Zhai, X. Yao, X.G. Cheng, L.Y. Zhang, H. Chen, Mater. Sci. Eng. B 94 (2002) 164–169.
[9] U.C. Chung, C. Elissalde, M. Maglione, C. Estournès, M. Paté, J.P. Ganne, Appl. Phys. Lett. 92 (2008) 042902–42903.
[10] J.D. Cui, G.X. Dong, Z.M. Yang, J. Du, J. Alloys Compd. 490 (2010) 353–357.
[11] S.M. Ke, H.T. Huang, H.Q. Fan, H.L.W. Chan, L.M. Zhou, Solid State Ionics 179 (2008) 1632–1635.
[12] S.M. Ke, H.Q. Fan, W. Wang, G.C. Jiao, H.T. Huang, H.L.W. Chan, Composites: Part A 39 (2008) 597–601.
[13] K.H. Yoon, J.C. Lee, J. Park, D.H. Kang, C.M. Song, Y.G. Seo, Jpn. J. Appl. Phys. 40 (2001) 5497–5500.
[14] F. Battllo, E. Duverger, J.C. Jules, J.C. Niepce, B. Jannot, M. Maglione, Ferroelectrics 109 (1990) 113–118.
[15] R.D. Shannon, Acta Cryst. A 32 (1976) 751–767.
[16] Z. Li, H.Q. Fan, Solid State Ionics 180 (2009) 1139–11142.
[17] L. Pauling, Proc. R. Soc. A 114 (1927) 191.
[18] Y. Chen, X.L. Dong, R.H. Liang, J.T. Li, Y.L. Wang, J. Appl. Phys. 98 (2005) 064107–64115.
[19] A.A. Bokov, I.P. Rayevskii, V.G. Smotrakov, O.I. Prokopalo, Phy. Status Solidi A 93 (1986) 411–417.